

3,5-Diphenyl-2-phosphafuran: Synthesis, Structure, and Thermally Reversible [4+2] Cycloaddition Chemistry

Martin-Louis Y. Riu and Christopher C. Cummins*

Department of Chemistry, Massachusetts Institute of Technology, Cambridge, MA 02139, USA

Received October 7, 2020; E-mail: ccummins@mit.edu

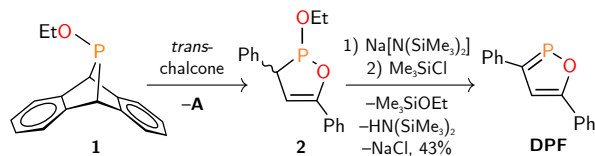
Abstract: Treatment of *trans*-chalcone with dibenzo-7-phosphanorbornadiene EtOPA (**A** = C₁₄H₁₀, anthracene), a source of ethoxyphosphinidene, followed by formal elimination of ethanol yields 3,5-diphenyl-2-phosphafuran (DPF) in 43% yield. We show that the phosphadiene moiety of DPF is a potent diene in the Diels–Alder reaction and reacts with dienophiles dimethylacetylene dicarboxylate (DPF-DMAD, 68%), norbornene (DPF-norbornene, 73%), and ethylene (DPF-C₂H₄, 80%) under ambient conditions. Mild heating of DPF-C₂H₄ results in the corresponding retro-Diels–Alder reaction, establishing DPF as a molecule that is able to reversibly bind ethylene.

In recent years, main group elements have been exploited for their “transition metal-like” properties and have been shown to react with catalytically relevant small molecules.^{1,2} In particular, reversible complexation of unsaturated molecules by main group species, previously thought to be the domain of transition metals, is a flourishing field in the current literature. Examples include ditetrelenes (RE≡ER, E = Ge, Sn),^{3–5} carbenes,⁶ tetrylenes (R₂E, E = Si, Ge, Sn)^{7–10} digallenanes,¹¹ magnesium(I) dimers,¹² and a number of boron^{13,14} and aluminum^{15–18} species.

Considering that replacement of carbon by phosphorus in unsaturated molecules yields energetically accessible frontier orbitals, due to the poor π overlap between the carbon and phosphorus centers,¹⁹ we targeted for synthesis a 2-phosphafuran to be tested for a possible ability to undergo low-barrier, thermally reversible cycloadditions. Such an ability would call to mind the thermally reversible cycloadditions between furan and maleimide moieties found in a number of self-healing polymers.^{20,21} While there are a number of reported phosphadienes that react with activated dienophiles, such as maleimide,^{22–25} examples of low-coordinate phosphorus species reversibly binding unsaturated molecules are rare.²⁶ Herein, we report the synthesis and characterization of a 2-phosphafuran that reversibly binds ethylene.

Heating a benzene solution of EtOPA (**1**)²⁷ and *trans*-chalcone to 80 °C for 4 h provided oxo-3-phospholene **2** as a mixture of diastereomers (³¹P NMR δ 180.6 and δ 170.9 ppm; *syn/anti* ratio 1.5:1; Scheme 1). The crude reaction mixture also contains small amounts of **1** and a tentatively assigned spirophosphorane byproduct (Fig. S.1). Attempts to separate **2** from this mixture by crystallization have been unsuccessful. In order to eliminate HOEt from **2**, compound **2** was first deprotonated with sodium bis(trimethylsilyl)amide (Na[N(SiMe₃)₂]) and the resulting in situ-generated, deep red anion was then treated with trimethylsilyl chloride (Me₃SiCl), providing 3,5-diphenyl-2-phosphafuran (DPF) upon elimination of HN(SiMe₃)₂,

NaCl, and Me₃SiOEt (Scheme 1). In agreement with a report of Mathey and co-workers,²⁸ DPF displays a notably deshielded ³¹P{¹H} NMR resonance of δ 285.4 ppm in benzene. Regitz and co-workers have also reported observation of a 2-phosphafuran by ³¹P NMR spectroscopy; however, the authors found it to be too labile for isolation.²⁹ Crystallization from minimal pentane at –35 °C provided DPF, as pale orange crystals, in 43% yield.



Scheme 1. Preparation of DPF Proceeded in Two Steps from EtOPA (**1**)

Crystals of DPF suitable for an X-ray diffraction study were grown from minimal diethyl ether at –35 °C, and the molecular structure of DPF is shown in Figure 1A. The experimental P–C bond length of 1.752(9) Å is between P–C single and double bond lengths (1.86 and 1.69 Å, respectively).³⁰ This bond length is consistent with moderate π -delocalization of the phosphaalkene double bond. A search of the Cambridge Structural Database returned no examples of 2-phosphafuran compounds with which to compare the structural data we obtained for DPF.

Bonding in DPF was investigated using natural resonance theory (NRT),^{31–33} a subroutine of natural bond orbital methods.³⁴ NRT-derived bond orders of 1.79 (C1–C3) and 1.80 (C2–P1) were found for DPF (Fig. 1B), values that are consistent with the intermediate bond lengths observed in the crystal structure of DPF. The dominant natural Lewis structures for the parent 2-phosphafuran were also determined, as depicted in Fig. 1C. The major resonance structure (63.2% contributor) for the parent molecule resembles a diene, involving localized C–C and C–P π -bonds, suggesting promise for Diels–Alder reactivity with dienophiles.

Quantum chemical calculations were employed to study the energy landscape of formation of the major isomer of compound **2** at the B3LYP-D3(BJ)/Def2-TZVPP level of DFT (Fig. 2). Calculations suggest that cheletropic addition of *trans*-chalcone to EtOPA (**1**), resulting in the formation of λ^5 -phosphorane **I1**, proceeds with an activation barrier of +24.7 kcal/mol (**TS1**). It should be noted that attempts to locate a local minimum for a possible zwitterionic product of conjugate addition consistently resulted in the convergence to **I1**. While formation of **I1** is thermodynamically favorable, this species was not observed by NMR spectroscopy. Our inability to observe this species is consistent with the small barrier (+6.3 kcal/mol) to anthracene fragmentation from this species, a process our computations suggest is

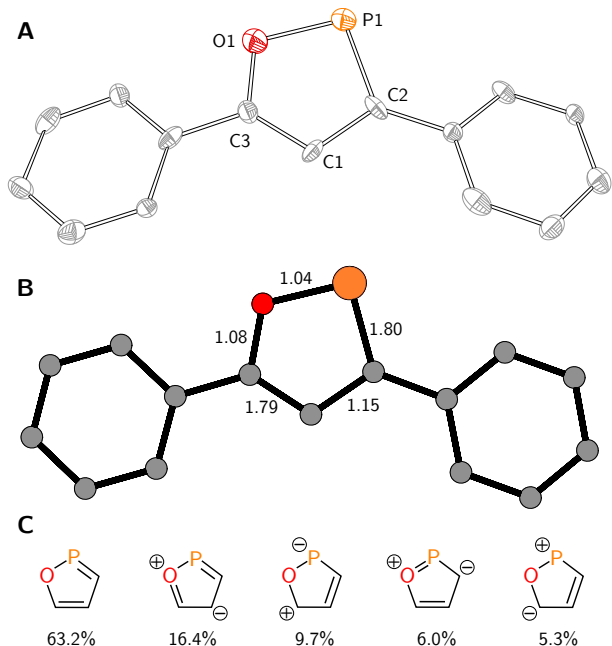
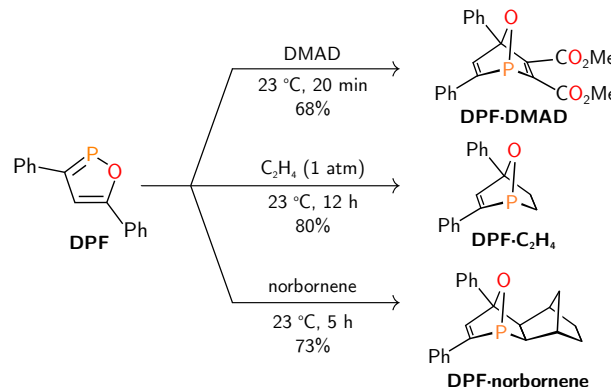


Figure 1. **A**) Molecular structure of DPF shown with 50% probability thermal ellipsoids. Hydrogen atoms are omitted for clarity. Selected bond lengths: P1–C2: 1.752(9) Å, C2–C1: 1.406(10) Å, C1–C3: 1.370(10) Å, C3–O1: 1.334(8) Å, O1–P1: 1.6745(17) Å. **B**) Natural resonance theory (NRT) derived bond orders for DPF. **C**) Resonance weight calculated for the parent 2-phosphafuran using NRT.

a concerted cheletropic extrusion pathway (**TS2**). Reductive elimination from λ^5 -phosphoranes, yielding a phosphorus(III) product, has been described previously.^{35–40}

Treatment of DPF with dimethylacetylene dicarboxylate (DMAD) at 23 °C results in the formation of DPF-DMAD (^{31}P NMR δ 95.3 ppm), and this adduct was isolated in 68% yield (Scheme 2). Colorless crystals of DPF-DMAD were grown from diethyl ether at –35 °C and structurally characterized in a single-crystal X-ray diffraction study (Fig. 3). Related 1-phosphanorbornadienes have been accessed by treating thermally generated 2*H*-phospholes with dienophiles.^{22–25}

Encouraged by the facile cycloaddition of DPF to DMAD, DPF was treated with ethylene. In contrast to the high temperatures and pressures often required for Diels–Alder



Scheme 2. Diels–Alder Adducts of DPF

addition of dienes to unactivated alkenes,⁴¹ complete conversion of DPF to DPF- C_2H_4 (^{31}P NMR δ 94.5 ppm) was observed 12 hours after exposure to ethylene (1 atm) at 23 °C (Scheme 2). Colorless crystals of DPF- C_2H_4 were grown from pentane at –35 °C in 80% yield. DPF- C_2H_4 was structurally characterized by X-ray crystallography and its molecular structure is shown in Fig. 3.

We also found that treatment of DPF with an excess of 1-hexene (10 equiv) led to partial conversion (ca. 64%) of DPF to the corresponding cycloadduct, as a mixture of diastereomers in a 3:8:25:62 molar ratio, after 12 h at 23 °C. However, no reaction was observed between DPF and unactivated internal olefins, such as cyclohexene and *cis*-4-octene, under similar conditions. Furthermore, no reaction was observed after heating a toluene solution of DPF and *cis*-4-octene (5 equiv) to 110 °C for 12 h.

Remarkably, when DPF- C_2H_4 was heated to 65 °C in tetrahydrofuran, formation of ethylene and DPF was observed by NMR spectroscopy. When this experiment was repeated at 75 °C in the presence of norbornene, clean formation of DPF-norbornene was observed after 15 h. To confirm the identity of the product, DPF-norbornene was prepared independently and obtained in 73% isolated yield (Scheme 2).

The reversible Diels–Alder reaction of DPF with ethylene prompted us to investigate the energy landscape of this reaction using quantum chemical calculations (Fig. 4). Calculations performed using DFT, at the $\omega\text{B97X-D3}/\text{Def2}$ -

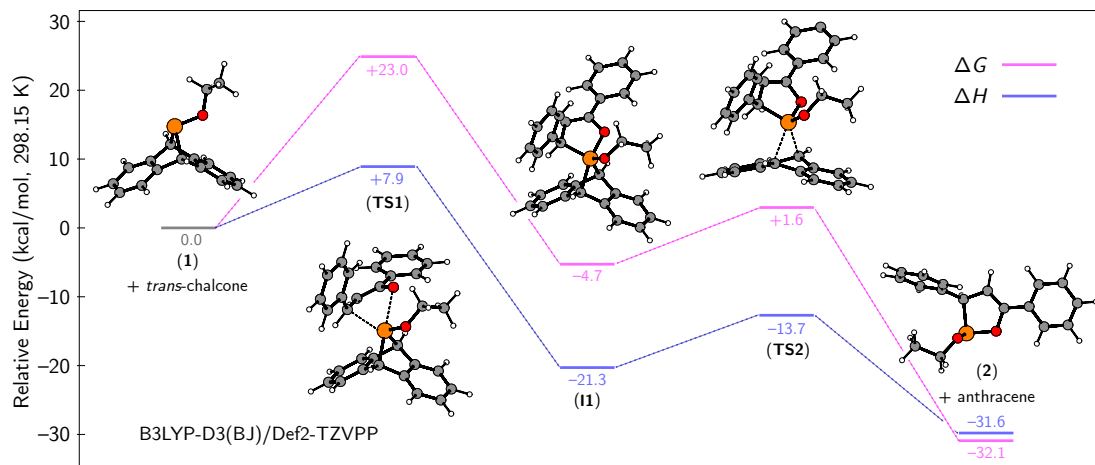


Figure 2. Minimum energy pathway for the reaction of EtOPA (1) with *trans*-chalcone to give compound 2.

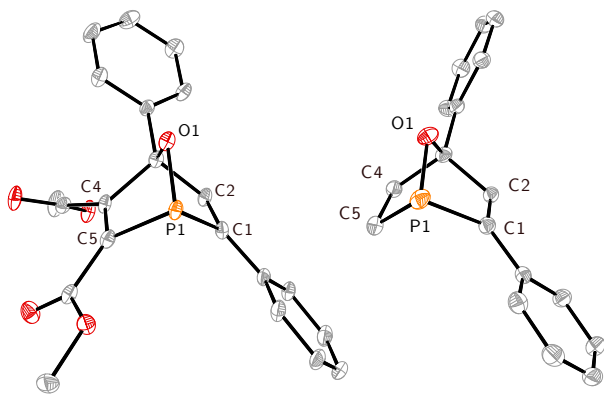


Figure 3. Molecular structure of cycloadducts DPF-DMAD (left) and DPF-C₂H₄ (right) shown with ellipsoids at the 50% probability level. Hydrogen atoms are omitted for clarity.

TZVPP level of theory, suggest that the cycloaddition is a concerted process, proceeding with an activation barrier of +26.5 kcal/mol (**TS**). These calculations also reveal that the reaction is enthalpically favorable ($\Delta H = -18.1$ kcal/mol) but is downhill by only -4.8 kcal/mol, consistent with the experimental observation of retrocyclization at elevated temperatures.

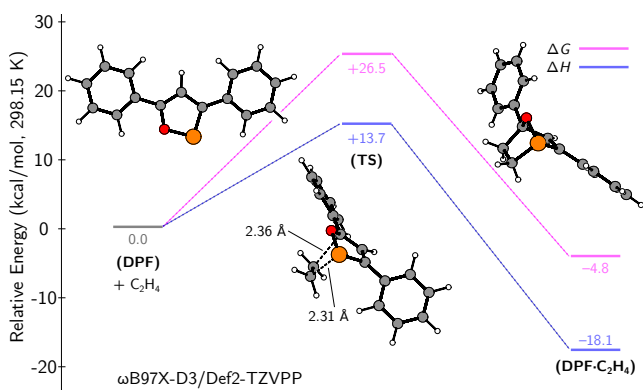


Figure 4. Calculated stationary points and transition state (“TS”) and their relative enthalpies (blue, kcal/mol) and free energies (pink, kcal/mol, 298.15 K) involved in the Diels–Alder addition of DPF to ethylene.

This work introduces 3,5-diphenyl-2-phosphafuran as a potent diene in the Diels–Alder reaction. DPF not only forms a cycloadduct with ethylene, but additionally, mild heating of DPF-C₂H₄ results in the retro-Diels–Alder reaction. Future work will involve the application of DPF as an olefin protecting group via the Diels–Alder reaction, a methodology that is largely absent from the literature due to the typically high temperatures required for cycloaddition and cyclereversion, especially in the case of an unactivated alkene as the dienophile.^{42–44}

Experimental Section

General Considerations. Except as otherwise noted, all manipulations were performed in a Vacuum Atmospheres model MO-40M glovebox under an inert atmosphere of purified N₂. All solvents were obtained anhydrous and oxygen-free by bubble degassing (Ar), purification by passage through columns of alumina using a solvent purification system (Pure Process Technology, Nashua, NH),⁴⁵ and storage over 4.0 Å molecular sieves.⁴⁶ Deuterated solvents were

purchased from Cambridge Isotope Labs, then degassed and stored over molecular sieves for at least 48 h prior to use. Celite (EM Science), 4.0 Å molecular sieves, silica, acidic alumina, and charcoal were dried by heating above 200 °C under dynamic vacuum (50 mTorr) for at least 48 h prior to use. All glassware was dried in an oven for at least two hours at temperatures greater than 150 °C.

1²⁷ was prepared according to a literature procedure. *Trans*-chalcone (Sigma-Aldrich), sodium bis(trimethylsilyl)amide (Sigma-Aldrich), norbornene (Alfa-Aesar), trimethylsilyl chloride (Fluka), ethylene (Airgas), and triphenylphosphine (Strem) were used as received. Dimethyl acetylenedicarboxylate (Alfa-Aesar), *cis*-4-octene (Sigma-Aldrich), 1-hexene (Sigma-Aldrich), and cyclohexene (Sigma-Aldrich) were distilled, degassed three times by the freeze-pump-thaw method, and stored over 4 Å molecular sieves for 48 h prior to use.

NMR spectra were obtained on a Jeol ECZ-500 instrument equipped with an Oxford Instruments superconducting magnet, on a Bruker Avance 400 instrument equipped with a Magnex Scientific or with a SpectroSpin superconducting magnet, or on a Bruker Avance 500 instrument equipped with a Magnex Scientific or with a SpectroSpin superconducting magnet. ¹H and ¹³C NMR spectra were referenced internally to residual solvent signals.⁴⁷ ³¹P NMR spectra were externally referenced to 85% H₃PO₄ (0 ppm). Structural assignments were made with additional information from gCOSY, gHSQC, gHMBC, and gNOESY experiments. Elemental combustion analyses were performed by Midwest Micro Laboratories (Indianapolis, IN, USA).

High resolution mass spectral (HRMS) data were collected using a Jeol AccuTOF 4G LC-Plus mass spectrometer equipped with an Ion-Sense DART source. Data were calibrated to a sample of PEG-600 and were collected in positive-ion mode. Samples were prepared in THF (10 μM concentration) and were briefly exposed to air (<5 s) before being placed in front of the DART source.

Synthesis of 2-Ethoxy-3,5-diphenyl-3-hydro-1,2-oxaphosphole (2). A solution of **1** (2.50 g, 9.84 mmol, 1.00 equiv) and *trans*-chalcone (2.05 g, 9.84 mmol, 1.00 equiv) in benzene (10 mL) was prepared in a 25 mL Schlenk tube containing a stir bar. The tube was removed from the glovebox and placed in an oil bath preheated to 80 °C. After 4 h, the flask was removed from the oil bath and allowed to cool for 30 min, during which time flakes of anthracene crystallized. The sealed tube was returned to the glovebox, where all volatile materials were removed *in vacuo*. To the residue was added Et₂O (15 mL) and the resulting slurry was filtered through a coarse sintered frit (15 mL) containing a one-inch plug of charcoal. The plug was washed with Et₂O (15 mL) and the combined filtrates were concentrated to ca. 5 mL under reduced pressure. The solution was then cooled to -35 °C in the glovebox freezer. After 24 h, the supernatant was decanted away from the white solids that had formed and all volatile materials were removed from the supernatant under reduced pressure. A pale yellow oil (2.41 g) comprising a mixture of **1**, *anti*-**2**, *syn*-**2**, and a tentatively assigned spirophosphorane byproduct (Fig. S.1), in a ca. 2.35:52:11 molar ratio, was obtained. The ratio of **1**, **2**, and spirophosphorane was determined by ³¹P{¹H} NMR spectroscopy. Attempts to remove EtOPA and the spirophosphorane byproduct from the mixture by crystallization have been unsuccessful. *anti*-**2**: DART HRMS(Q-TOF) m/z: [M+H]⁺ Calcd for C₁₇H₁₈O₂P 285.1044; Found

285.1063. ^1H NMR (400 MHz, chloroform-*d*, 25 °C): δ 7.81-7.09 (aryl, 10H), 5.94 (dd, J = 9.3, 3.7 Hz, 1H), 4.13 (t, J = 3.6 Hz, 1H), 4.01 (m, 2H), 1.33 (t, J = 7.1 Hz, 3H). $^{13}\text{C}\{\text{H}\}$ NMR (101 MHz, chloroform-*d*, 25 °C): δ 157.6 (d, $^2J_{\text{PC}}$ = 7.3 Hz), 138-123 (aryl), 102.2, 64.7 (d, $^1J_{\text{PC}}$ = 19.3 Hz), 57.8 (d, $^2J_{\text{PC}}$ = 26.7 Hz), 17.4 (d, $^3J_{\text{PC}}$ = 5.3 Hz) ppm. $^{31}\text{P}\{\text{H}\}$ NMR (162 MHz, chloroform-*d*, 25 °C): δ 180.3 ppm. *syn-2*: DART HRMS(Q-TOF) m/z: [M+H]⁺ Calcd for $\text{C}_{17}\text{H}_{18}\text{O}_2\text{P}$ 285.1044; Found 285.1063. ^1H NMR (400 MHz, chloroform-*d*, 25 °C): δ 7.81-7.09 (aryl, 10H), 5.85 (dd, J = 8.6, 2.5 Hz, 1H), 4.45 (dd, J = 31.9, 2.5 Hz, 1H), 3.88-3.59 (m, 2H), 0.88 (t, J = 7.0 Hz, 3H). $^{13}\text{C}\{\text{H}\}$ NMR (101 MHz, chloroform-*d*, 25 °C): δ 157.7 (d, $^2J_{\text{PC}}$ = 6.8 Hz), 138-123 (aryl), 101.6, 64.3 (d, $^1J_{\text{PC}}$ = 11.8 Hz), 58.9 (d, $^2J_{\text{PC}}$ = 26.0 Hz), 16.8 (d, $^3J_{\text{PC}}$ = 5.2 Hz) ppm. $^{31}\text{P}\{\text{H}\}$ NMR (162 MHz, chloroform-*d*, 25 °C): δ 170.5 ppm.

Synthesis of 3,5-Diphenyl-2-phosphafuran (DPF). To a thawing solution of crude **2** (0.500 g, 1.76 mmol, 1.00 equiv; the amount weighed out depends on the composition of the crude starting material) in 1,2-dimethoxyethane (20 mL), was added sodium bis(trimethylsilyl)amide (0.323 g, 1.76 mmol, 1.00 equiv) portionwise. After vigorously stirring for 15 min, the deep red solution was frozen in the glovebox coldwell. To the thawing solution was added trimethylsilyl chloride (0.192 g, 1.76 mmol, 1.00 equiv) dropwise. Following the addition, the mixture was stirred as it warmed to 23 °C over one hour. During this period the reaction mixture became cloudy and bright orange. All volatile materials were removed *in vacuo*, and the resulting bright orange solids were taken up in pentane (10 mL) and the solution was filtered through a 15 mL coarse sintered frit containing a two-inch plug of Celite. The Celite plug was washed with additional pentane (10 mL) and all volatile materials were removed from the combined filtrates *in vacuo*, yielding a deep orange residue. Crystallization from minimal pentane at -35 °C provided DPF as a pale orange crystalline material (0.180 g, 1.51 mmol, 43%). Melting point: 82-83 °C. DART HRMS(Q-TOF) m/z: [M+H]⁺ Calcd for $\text{C}_{15}\text{H}_{12}\text{OP}$ 239.0626; Found 239.0620. Anal. Calcd for $\text{C}_{15}\text{H}_{11}\text{OP}$: C, 75.21; H, 4.77; N, 0. Found: C, 75.63; H 4.65; N, 0. ^1H NMR (400 MHz, chloroform-*d*, 25 °C): δ 7.84 (d, J = 7.8 Hz, 2H), 7.61 (d, J = 7.6 Hz, 2H), 7.49 (d, $^3J_{\text{PH}}$ = 8.8 Hz, 1H), 7.44 (m, 4H), 7.35 (m, 2H) ppm. $^{13}\text{C}\{\text{H}\}$ NMR (101 MHz, chloroform-*d*, 25 °C): δ 180.6 (d, J = 52.0 Hz), 167.5, 134.2 (d, J = 14.2 Hz), 132.2 (d, J = 5.0 Hz), 129.3, 129.0 (d, J = 1.2 Hz), 128.7 (d, J = 2.6 Hz), 128.7 (d, J = 3.0 Hz), 126.1 (d, J = 11.8 Hz), 125.1 (d, J = 1.9 Hz), 110.7 (d, J = 2.8 Hz) ppm. $^{31}\text{P}\{\text{H}\}$ NMR (162 MHz, chloroform-*d*, 25 °C): δ 284.6 (d, $^3J_{\text{PH}}$ = 8.8 Hz) ppm.

Synthesis of Dimethyl-4,6-diphenyl-7-oxa-1-phosphabicyclo[2.2.1]hepta-2,5-diene-2,3-dicarboxylate (DPF-DMAD). A solution of dimethyl acetylenedicarboxylate (0.119 g, 0.840 mmol, 1.00 equiv) in THF (2 mL) was added dropwise to a stirring solution of DPF (0.200 g, 0.840 mmol, 1.00 equiv) in THF (5 mL). After vigorous stirring for 20 min, all volatile materials were removed *in vacuo* from the reaction mixture. A white heterogeneous mixture was obtained after adding pentane (10 mL) to the resulting colorless residue and stirring the solution for 20 min. The white precipitate was collected by vacuum filtration using a 15 mL coarse sintered frit and the solids were washed with minimal pentane (ca. 2 × 5 mL) and dried to constant mass under reduced pressure. Crystallization from minimal diethyl ether at -35 °C provided colorless crys-

tals of DPF-DMAD (0.217 g, 0.571 mmol, 68%). Melting point: 95-96 °C dec. DART HRMS(Q-TOF) m/z: [M+H]⁺ Calcd for $\text{C}_{21}\text{H}_{18}\text{O}_5\text{P}$ 381.0892; Found 381.0897. ^1H NMR (500 MHz, chloroform-*d*, 25 °C): δ 7.84 (d, J = 9.0 Hz, 1H), 7.64-7.61 (m, 3H), 7.55 (d, J = 8.0 Hz, 2H), 7.45 (t, J = 7.2 Hz, 2H), 7.43-7.38 (m, 3H), 7.35 (t, J = 7.3 Hz, 1H), 3.79 (s, 3H), 3.61 (s, 3H) ppm. $^{13}\text{C}\{\text{H}\}$ NMR (126 MHz, chloroform-*d*, 25 °C): δ 166.7 (d, J = 35.3 Hz), 166.2 (d, J = 2.9 Hz), 163.9 (d, J = 17.8 Hz), 163.9 (d, J = 3.2 Hz), 153.3 (d, J = 41.7 Hz), 139.1 (d, J = 2.0 Hz), 134.9, 134.1 (d, J = 17.8 Hz), 129.4, 129.3, 129.2, 128.9, 126.7, 126.4, 108.0 (d, J = 12.1 Hz), 52.7, 52.6 ppm. $^{31}\text{P}\{\text{H}\}$ NMR (203 MHz, chloroform-*d*, 25 °C): δ 95.4 ppm.

Synthesis of 2,4-Diphenyl-7-oxa-1-phosphabicyclo[2.2.1]hepta-2-ene (DPF-C₂H₄). A solution of DPF (100 mg, 0.42 mmol, 1 equiv) in THF (3 mL) was prepared in the glovebox and transferred to a sealed 25 mL Schlenk tube containing a stir bar. The tube was removed from the glovebox and degassed by three freeze-pump-thaw cycles and back-filled with ethylene (1.0 atm, 1.1 mmol, 0.031 g). After vigorously stirring for 12 h, the sealed tube was returned to the glovebox, where all volatile materials were removed *in vacuo*. Pentane (10 mL) was added to the pale brown residue and the resulting solution was filtered through a 15 mL coarse sintered frit containing a one-inch plug of Celite. The plug was washed with additional pentane (5 mL) and all volatile materials were removed from the combined filtrates under reduced pressure. Crystallization from minimal diethyl ether at -35 °C provided colorless crystals of DPF-C₂H₄ (0.089 g, 0.33 mmol, 80%). Melting point 74-75 °C. Anal. Calcd for $\text{C}_{17}\text{H}_{15}\text{OP}$: C, 76.75; H 5.68, N 0. Found: C, 76.68; H, 5.12; N, 0. ^1H NMR (500 MHz, chloroform-*d*, 25 °C): δ 7.60 (d, J = 7.3 Hz, 2H), 7.49 (d, J = 7.8 Hz, 2H), 7.44 (t, J = 7.6 Hz, 2H), 7.38-7.32 (m, 3H), 7.32-7.24 (m, 1H), 6.90 (d, J = 9.1 Hz, 1H), 2.21 (qd, J = 11.4, 2.3 Hz, 1H), 1.97-1.87 (m, 1H), 1.88-1.76 (m, 1H), 1.44-1.32 (m, 1H) ppm. $^{13}\text{C}\{\text{H}\}$ NMR (126 MHz, chloroform-*d*, 25 °C): δ 153.3 (d, J = 29.3 Hz), 140.6, 137.8, 134.1 (d, J = 16.8 Hz), 129.0, 128.7, 128.4, 128.0, 126.9 (d, J = 8.9 Hz), 125.8, 100.8 (d, J = 11.7 Hz), 28.4, 25.7 (d, J = 21.0 Hz). $^{31}\text{P}\{\text{H}\}$ NMR (202 MHz, chloroform-*d*, 25 °C): δ 95.6 ppm.

Synthesis of (±)-(1*R*,2*R*,3*S*,6*R*,7*R*,8*S*)-8,10-diphenyl-11-oxa-1-phosphatetracyclo[6.2.1.1^{3,6}.0².7]dodec-9-ene (DPF-norbornene). Norbornene (0.040 g, 0.42 mmol, 1.0 equiv) was added to a solution of DPF (0.100 g, 0.420 mmol, 1.00 equiv) in THF (4 mL) portionwise. After vigorous stirring for 5 h, all volatile materials were removed *in vacuo*, resulting in a colorless residue. Pentane (10 mL) was added to this residue and the resulting solution was filtered through a 15 mL coarse sintered frit containing a one-inch plug of Celite. The plug was washed with additional pentane (5 mL) and all volatile materials were removed from the combined filtrates *in vacuo*. Crystallization from minimal pentane at -35 °C provided colorless crystals of DPF-norbornene (0.102 g, 0.31 mmol, 73%). Melting point 110-111 °C. Anal. Calcd for $\text{C}_{22}\text{H}_{21}\text{OP}$: C, 79.88; H, 6.19; N, 0. Found: C, 79.50; H, 6.37; N, 0. ^1H NMR (500 MHz, chloroform-*d*, 25 °C): δ 7.55 (d, J = 7.4 Hz, 2H), 7.45 (t, J = 7.4 Hz, 2H), 7.43 (d, J = 6.3 Hz, 2H), 7.34 (t, J = 7.4 Hz, 3H), 7.29-7.24 (m, 1H), 6.96 (d, J = 9.2 Hz, 1H), 2.63 (br, 1H), 1.92 (dd, J = 6.3, 1.7 Hz, 1H), 1.86 (d, J = 9.9 Hz, 1H), 1.81-1.76 (m, 2H), 1.61-1.49 (m, 1H), 1.44-1.34 (m, 1H), 1.24-1.15 (m, 1H), 1.09-1.00 (m, 1H), 0.82 (d, J = 9.8 Hz, 1H) ppm. $^{13}\text{C}\{\text{H}\}$ NMR (126 MHz,

chloroform-*d*, 25 °C): δ 152.4 (d, J = 28.4 Hz), 140.4, 139.6, 134.4 (d, J = 16.9 Hz), 128.9, 128.5, 128.3, 127.3, 126.8 (d, J = 8.7 Hz), 125.7, 102.8 (d, J = 10.2 Hz) 51.1 (d, J = 22.5 Hz), 50.3 (d, J = 2.4 Hz), 39.5 (d, J = 13.3 Hz), 37.1, 34.1, 30.8 (d, J = 10.1 Hz), 30.2 ppm. $^{31}\text{P}\{\text{H}\}$ NMR (202 MHz, chloroform-*d*, 25 °C): δ 101.7 ppm.

Air Stability of DPF. A 0.02 M solution of DPF in benzene-*d*₆ was prepared and transferred to an NMR tube. To this tube was added a glass capillary containing a 0.67 M solution of triphenylphosphine in benzene-*d*₆ and initial NMR spectra were collected (Fig. S.36 and S.37). The cap of the tube was removed outside of the glovebox and after 1 h the solution became pale yellow. NMR spectra of this sample were collected and the spectra are depicted in Fig. S.38 and S.39. Complete consumption of DPF and no new resonances were observed by $^{31}\text{P}\{\text{H}\}$ NMR spectroscopy. The fate of DPF under these conditions is not yet known.

Thermal Stability of DPF·C₂H₄. A 0.03 M solution of DPF·C₂H₄ in THF was prepared in the glovebox and transferred to a J Young tube containing a flame-sealed glass capillary charged with a 0.67 M benzene-*d*₆ solution of triphenylphosphine. An initial $^{31}\text{P}\{\text{H}\}$ NMR spectrum of the solution was collected (Fig. S.40). The tube was then placed in a preheated 65 °C oil bath and NMR spectra of the solution were collected after 4 h (Fig. S.41). Partial conversion of DPF·C₂H₄ to DPF was observed, as assessed by $^{31}\text{P}\{\text{H}\}$ NMR spectroscopy, and a resonance assigned to ethylene (δ 5.34 ppm) was present in the ¹H NMR spectrum (Fig. S.42).

Thermolysis of DPF·C₂H₄ in the Presence of Norbornene. A solution of DPF·C₂H₄ (10 mg, 0.038 mmol, 1.0 equiv) and norbornene (4 mg, 0.04 mmol, 1 equiv) in THF (0.7 mL) was prepared in the glovebox and transferred to a J Young tube containing a flame-sealed glass capillary charged with a 0.67 M benzene-*d*₆ solution of triphenylphosphine. An initial $^{31}\text{P}\{\text{H}\}$ NMR spectrum of the solution was collected (Fig. S.43). The tube was then placed in a preheated 75 °C oil bath and $^{31}\text{P}\{\text{H}\}$ NMR spectra of the solution were collected after 3 and 15 h (Fig. S.44 and S.45). Clean formation of DPF·norbornene was observed.

Treatment of DPF with 1-Hexene. A solution of DPF (10 mg, 0.038 mmol, 1.0 equiv) and 1-hexene (32 mg, 0.38 mmol, 10 equiv) in benzene-*d*₆ (0.7 mL) was prepared in the glovebox and transferred to a NMR tube containing a flame-sealed glass capillary charged with a 0.67 M benzene-*d*₆ solution of triphenylphosphine. A $^{31}\text{P}\{\text{H}\}$ NMR spectrum of the solution was collected after 12 h (Fig. S.46). Partial conversion (ca. 64%) of DPF to the corresponding cycloadduct, as a mixture of diastereomers in a 3:8:25:62 molar ratio, was observed. Due to overlapping signals in ¹H NMR spectrum, we are unable to assign the stereochemistry of the cycloadducts. Attempts to separate the cycloadducts by crystallization have been unsuccessful.

X-Ray Diffraction Studies. Low-temperature diffraction data were collected on a Bruker-AXS X8 Kappa Duo diffractometer with $I\mu\text{S}$ micro-sources, coupled to a Photon 3 CPAD detector using Mo K_{α} radiation (λ = 0.71073 Å) for the structure of DPF·DMAD and a Smart APEX2 CCD detector using Mo K_{α} radiation (λ = 0.71073 Å) for the structures of DPF and DPF·C₂H₄, performing ϕ - and ω -scans. The structures were solved by dual-space methods using SHELXT⁴⁸ and refined against F^2 on all data by full-matrix least squares with SHELXL-2017⁴⁸ following established refinement strategies.^{49,50} All non-hydrogen atoms

were refined anisotropically. All hydrogen atoms were included into the model at geometrically calculated positions and refined using a riding model. The isotropic displacement parameters of all hydrogen atoms were fixed to 1.2 times the U-value of the atoms they are linked to (1.5 times for methyl groups). Descriptions of the individual refinements follow below and details of the data quality and a summary of the residual values of the refinements for all structures are given in Table S.1 and S.2. Further details can be found in the form of .cif files available from the CCDC.

Single crystals of DPF were grown were grown from -35 °C pentane. The structure was solved in the orthorhombic space group *Pnma* with half a molecule of DPF and no solvent molecules in the asymmetric unit. The structure exhibits whole molecule disorder about a crystallographic inversion center. Disorders were refined with the help of the FLAT restraint in SHELXL and similarity restraints on 1,2 and 1,3 distances. Similarity and rigid bond restraints for anisotropic displacement parameters were applied to all non-hydrogen atoms.

Single crystals of DPF·DMAD were grown from -35 °C diethyl ether. The structure was solved in the monoclinic space group *P2₁/c* with one molecule of DPF·DMAD and no solvent molecules in the asymmetric unit. The molecule exhibits no disorder. Similarity and rigid bond restraints for anisotropic displacement parameters were applied to all non-hydrogen atoms.

Single crystals of DPF·C₂H₄ were grown from -35 °C diethyl ether. The structure was solved in the monoclinic space group *P2₁/n* with one molecule of DPF·C₂H₄ and no solvent molecules in the asymmetric unit. The molecule exhibits no disorder. Similarity and rigid bond restraints for anisotropic displacement parameters were applied to all non-hydrogen atoms.

Computational Studies. All calculations were performed with the ORCA 4.0.1 quantum chemistry package from the development team at the University of Bonn.^{51,52} Initial geometries were constructed in Avogadro.^{53,54} Geometry optimizations were performed at the *wB97X-D3/Def2-TZVPP* level of theory using keywords *wB97X-D3 def2-TZVPP def2/J TightSCF RIJCOSX Grid4 FinalGrid5 Opt* for the geometries listed in S.4.1–S.4.7 and at the *B3LYP-D3(BJ)/Def2-TZVPP* using keywords *B3LYP D3BJ Def2-TZVPP TightSCF RIJCOSX Grid4 FinalGrid5 Opt* for the geometries listed in S.4.8–S.4.12. For transition states, the keyword *Opt* was replaced by *OptTS*. Vibrational frequency calculations were carried out on the optimized geometries using the keyword *NumFreq*. Intermediate and transition state geometries were found to have zero and one imaginary frequency, respectively. Natural bond orbital (NBO) calculations were performed using NBO6³⁴ within the ORCA program. The natural resonance theory (NRT) keyword was specified to generate natural resonance structures of the parent 2-phosphafuran molecule. Lower contributing resonance structures (all below 5%) were not included in the main text.

Supporting Information. NMR spectra of new compounds and reactivity studies, X-ray crystallographic data, and computational details. FAIR Data is available as Supporting Information for Publication and includes the primary NMR FID files for compounds **2**, DPF, DPF·DMAD, DPF·C₂H₄, and DPF·norbornene.

Competing Interest: The authors declare no competing interest.

Acknowledgements: We thank Michael B. Geeson, Wesley J. Transue, and Scott M. Shepard for thoughtful discussions and suggestions. This material is based on research supported by the National Science Foundation under CHE-1955612.

References

- Power, P. P. Main-group elements as transition metals. *Nature* **2010**, *463*, 171–177, DOI: 10.1038/nature08634.
- Martin, D.; Soleilhavoup, M.; Bertrand, G. Stable singlet carbenes as mimics for transition metal centers. *Chem. Sci.* **2011**, *2*, 389–399, DOI: 10.1039/C0SC00388C.
- Peng, Y.; Ellis, B. D.; Wang, X.; Fettinger, J. C.; Power, P. P. Reversible Reactions of Ethylene with Distannynes Under Ambient Conditions. *Science* **2009**, *325*, 1668–1670, DOI: 10.1126/science.1176443.
- Hadlington, T. J.; Li, J.; Hermann, M.; Davey, A.; Frenking, G.; Jones, C. Reactivity of Amido-Digermynes, LGeGeL (L = Bulky Amide), toward Olefins and Related Molecules: Facile Reduction, C–H Activation, and Reversible Cycloaddition of Unsaturated Substrates. *Organometallics* **2015**, *34*, 3175–3185, DOI: 10.1021/acs.organomet.5b00206.
- Sugahara, T.; Guo, J.-D.; Sasamori, T.; Nagase, S.; Tokitoh, N. Reversible addition of terminal alkenes to digermynes. *Chem. Commun.* **2018**, *54*, 519–522, DOI: 10.1039/C7CC08555A.
- Moerdyk, J. P.; Bielawski, C. W. Diamidocarbenes as versatile and reversible [2 + 1] cycloaddition reagents. *Nat. Chem.* **2012**, *4*, 275–280, DOI: 10.1038/nchem.1267.
- Rodriguez, R.; Gau, D.; Kato, T.; Saffon-Merceron, N.; De Cárz, A.; Cossío, F. P.; Baceiredo, A. Reversible Binding of Ethylene to Silylene–Phosphine Complexes at Room Temperature. *Angew. Chem. Int. Ed.* **2011**, *50*, 10414–10416, DOI: 10.1002/anie.201105097.
- Lips, F.; Fettinger, J. C.; Mansikkamäki, A.; Tuunonen, H. M.; Power, P. P. Reversible Complexation of Ethylene by a Silylene under Ambient Conditions. *J. Am. Chem. Soc.* **2014**, *136*, 634–637, DOI: 10.1021/ja411951y.
- Lai, T. Y.; Gullett, K. L.; Chen, C.-Y.; Fettinger, J. C.; Power, P. P. Reversible Complexation of Alkynes by a Germylene. *Organometallics* **2019**, *38*, 1421–1424, DOI: 10.1021/acs.organomet.9b00077.
- Sita, L. R.; Bickerstaff, R. D. Synthesis and crystal structure of the first stannacyclop propane derivative. *J. Am. Chem. Soc.* **1988**, *110*, 5208–5209, DOI: 10.1021/ja00223a059.
- Caputo, C. A.; Guo, J.-D.; Nagase, S.; Fettinger, J. C.; Power, P. P. Reversible and Irreversible Higher-Order Cycloaddition Reactions of Polyolefins with a Multiple-Bonded Heavier Group 13 Alkene Analogue: Contrasting the Behavior of Systems with π - π , π - π^* and π -n₊ Frontier Molecular Orbital Symmetry. *J. Am. Chem. Soc.* **2012**, *134*, 7155–7164, DOI: 10.1021/ja301247h.
- Boutland, A. J.; Carroll, A.; Alvarez Lamsfus, C.; Stasch, A.; Maron, L.; Jones, C. Reversible Insertion of a C=C Bond into Magnesium(I) Dimers: Generation of Highly Active 1,2-Dimagnesioethane Compounds. *J. Am. Chem. Soc.* **2017**, *139*, 18190–18193, DOI: 10.1021/jacs.7b11368.
- Wu, D.; Ganguly, R.; Li, Y.; Hoo, S. N.; Hirao, H.; Kinjo, R. Reversible [4 + 2] cycloaddition reaction of 1,3,2,5-diazidoborinime with ethylene. *Chem. Sci.* **2015**, *6*, 7150–7155, DOI: 10.1039/C5SC03174E.
- Taylor, J. W.; McSkimming, A.; Guzman, C. F.; Harman, W. H. N-Heterocyclic Carbene-Stabilized Boranthrene as a Metal-Free Platform for the Activation of Small Molecules. *J. Am. Chem. Soc.* **2017**, *139*, 11032–11035, DOI: 10.1021/jacs.7b06772.
- Radzewich, C. E.; Coles, M. P.; Jordan, R. F. Reversible Ethylene Cycloaddition Reactions of Cationic Aluminum β -Diketiminate Complexes. *J. Am. Chem. Soc.* **1998**, *120*, 9384–9385, DOI: 10.1021/ja9818405.
- Bakewell, C.; White, A. J. P.; Crimmin, M. R. Reactions of Fluoroalkenes with an Aluminum(I) Complex. *Angew. Chem. Int. Ed.* **2018**, *57*, 6638–6642, DOI: 10.1002/anie.201802321.
- Schwamm, R. J.; Anker, M. D.; Lein, M.; Coles, M. P. Reduction vs. Addition: The Reaction of an Aluminyl Anion with 1,3,5,7-Cyclooctatetraene. *Angew. Chem. Int. Ed.* **2019**, *58*, 1489–1493, DOI: 10.1002/anie.201811675.
- Bakewell, C.; White, A. J. P.; Crimmin, M. R. Reversible alkene binding and allylic C–H activation with an aluminum(I) complex. *Chem. Sci.* **2019**, *10*, 2452–2458, DOI: 10.1039/C8SC04865G.
- Kutzelnigg, W. Chemical Bonding in Higher Main Group Elements. *Angew. Chem. Int. Ed.* **1984**, *23*, 272–295, DOI: 10.1002/anie.198402721.
- Chen, X.; Dam, M. A.; Ono, K.; Mal, A.; Shen, H.; Nutt, S. R.; Sheran, K.; Wudl, F. A Thermally Re-mendable Cross-Linked Polymeric Material. *Science* **2002**, *295*, 1698–1702, DOI: 10.1126/science.1065879.
- Liu, Y.-L.; Chuo, T.-W. Self-healing polymers based on thermally reversible Diels–Alder chemistry. *Polym. Chem.* **2013**, *4*, 2194–2205, DOI: 10.1039/C2PY20957H.
- Mathey, F.; Mercier, F.; Charrier, C.; Fischer, J.; Mitschler, A. Dicoordinated 2H-phospholes as transient intermediates in the reactions of tervalent phospholes at high temperature. One-step syntheses of 1-phanorbornadienes and phosphorins from phospholes. *J. Am. Chem. Soc.* **1981**, *103*, 4595–4597, DOI: 10.1021/ja00405a058.
- Charrier, C.; Bonnard, H.; De Lauzon, G.; Mathey, F. Proton [1,5] shifts in P-unsubstituted 1H-phospholes. Synthesis and chemistry of 2H-phosphole dimers. *J. Am. Chem. Soc.* **1983**, *105*, 6871–6877, DOI: 10.1021/ja00361a022.
- Le Goff, P.; Mathey, F.; Ricard, L. [4 + 2] Cycloadditions between 2H-phospholes and alkenes. Synthesis and properties of 1-phanorbornenes. *J. Org. Chem.* **1989**, *54*, 4754–4758, DOI: 10.1021/jo00281a013.
- Mathey, F. Transient 2H-Phospholes as Powerful Synthetic Intermediates in Organophosphorus Chemistry. *Acc. Chem. Res.* **2004**, *37*, 954–960, DOI: 10.1021/ar030118v.
- Courtemanche, M.-A.; Transue, W. J.; Cummins, C. C. Phosphinidene Reactivity of a Transient Vanadium P≡N Complex. *J. Am. Chem. Soc.* **2016**, *138*, 16220–16223, DOI: 10.1021/jacs.6b10545.
- Transue, W. J.; Velian, A.; Nava, M.; García-Iriepa, C.; Temprado, M.; Cummins, C. C. Mechanism and Scope of Phosphinidene Transfer from Dibenzo-7-phosphorbornadiene Compounds. *J. Am. Chem. Soc.* **2017**, *139*, 10822–10831, DOI: 10.1021/jacs.7b05464.
- Duffy, M. P.; Lin, Y.; Ho, F.; Mathey, F. Synthesis and Chemistry of 2-Phosphafurans. *Organometallics* **2010**, *29*, 5757–5758, DOI: 10.1021/om100778f.
- Mack, A.; Bergsträßer, U.; Reiß, G. J.; Regitz, M. 3,5-Dimesityl-1,2,4-oxadiaphosphole – Synthesis and Reactivity of a Novel Heterocycle. *Eur. J. Org. Chem.* **1999**, 587–595.
- Pyykkö, P.; Atsumi, M. Molecular Double-Bond Covalent Radii for Elements Li–E112. *Chem. Eur. J.* **2009**, *15*, 12770–12779, DOI: 10.1002/chem.200901472.
- Glendening, E. D.; Weinhold, F. Natural resonance theory: I. General formalism. *J. Comput. Chem.* **1998**, *19*, 593–609.
- Glendening, E. D.; Weinhold, F. Natural resonance theory: II. Natural bond order and valency. *J. Comput. Chem.* **1998**, *19*, 610–627.
- Glendening, E. D.; Badenhoop, J. K.; Weinhold, F. Natural resonance theory: III. Chemical applications. *J. Comput. Chem.* **1998**, *19*, 628–646.
- Glendening, E. D.; Badenhoop, J. K.; Reed, A. E.; Carpenter, J. E.; Bohmann, J. A.; Morales, C. M.; Landis, C. R.; Weinhold, F. NBO 6.0 (Theoretical Chemistry Institute, University of Wisconsin, Madison, 2013).
- Mesch, K. A.; Quin, D. Syn to Anti Isomerization and Degradation of Phosphines of the 7-Phosphorbornene System by Action of Methanol. *Tetrahedron Lett.* **1980**, *21*, 4791–4794, DOI: 10.1016/0040-4039(80)80141-9.
- Newkome, G. R.; Hager, D. C. A new contractive coupling procedure. Convenient phosphorus expulsion reaction. *J. Am. Chem. Soc.* **1978**, *100*, 5567–5568, DOI: 10.1021/ja00485a053.
- Uchida, Y.; Onoue, K.; Tada, N.; Nagao, F.; Oae, S. Ligand coupling reaction on the phosphorus atom. *Tetrahedron Lett.* **1989**, *30*, 567–570, DOI: 10.1016/S0040-4039(00)95256-0.
- Uchida, Y.; Kozawa, H. Formation of 2,2-bipyridyl by ligand coupling on the phosphorus atom. *Tetrahedron Lett.* **1989**, *30*, 6365–6368, DOI: 10.1016/S0040-4039(01)93895-X.
- Hilton, M. C.; Zhang, X.; Boyle, B. T.; Alegre-Requena, J. V.; Paton, R. S.; McNally, A. Heterobiaryl synthesis by contractive C–C coupling via P(V) intermediates. *Science* **2018**, *362*, 799–804, DOI: 10.1126/science.aas8961.
- Szkop, K. M.; Geeson, M. B.; Stephan, D. W.; Cummins, C. C. Synthesis of acyl(chloro)phosphines enabled by phosphinidene transfer. *Chem. Sci.* **2019**, *10*, 3627–3631, DOI: 10.1039/C8SC05657A.
- Sauer, J.; Sustmann, R. Mechanistic Aspects of Diels–Alder Reactions: A Critical Survey. *Angew. Chem. Int. Ed.* **1980**, *19*, 779–807, DOI: 10.1002/anie.198007791.
- Tobia, D.; Harrison, R.; Phillips, B.; White, T. L.; DiMare, M.; Rickborn, B. Unusual stability of N-methylmaleimide cycloadducts: characterization of isobenzofuran retro-Diels–Alder reactions. *J. Org. Chem.* **1993**, *58*, 6701–6706, DOI: 10.1021/jo00076a032.
- Bunnage, M. E.; Nicolaou, K. C. The Oxide Anion Accelerated Retro-Diels–Alder Reaction. *Chem. Eur. J.* **1997**, *3*, 187–192, DOI: 10.1002/chem.19970030204.
- Kotha, S.; Banerjee, S. Recent developments in the retro-Diels–Alder reaction. *RSC Adv.* **2013**, *3*, 7642–7666, DOI: 10.1039/c3ra22762f.
- Pangborn, A. B.; Giardello, M. A.; Grubbs, R. H.; Rosen, R. K.; Timmers, F. J. Safe and Convenient Procedure for Solvent Purification. *Organometallics* **1996**, *15*, 1518–1520, DOI: 10.1021/oм9503712.
- Williams, D. B. G.; Lawton, M. Drying of Organic Solvents: Quantitative Evaluation of the Efficiency of Several Desiccants. *J. Org. Chem.* **2010**, *75*, 8351–8354, DOI: 10.1021/jo101589h.
- Fulmer, G. R.; Miller, A. J. M.; Sherdon, N. H.; Gottlieb, H. E.; Nudelman, A.; Stoltz, B. M.; Bercaw, J. E.; Goldberg, K. I. NMR Chemical Shifts of Trace Impurities: Common Laboratory Solvents, Organics, and Gases in Deuterated Solvents Relevant to the Organometallic Chemist. *Organometallics* **2010**, *29*, 2176–2179, DOI: 10.1021/oм100106e.

(48) Sheldrick, G. M. SHELXT – Integrated space-group and crystal-structure determination. *Acta Cryst. A* **2015**, *71*, 3–8, DOI: 10.1107/S2053273314026370.

(49) Müller, P.; Herbst-Irmer, R.; Spek, A. L.; Schneider, T. R.; Sawaya, M. R. *Crystal Structure Refinement: A Crystallographer's Guide to SHELXL*; IUCr Texts on Crystallography; Oxford University Press: Oxford, 2006.

(50) Müller, P. Practical suggestions for better crystal structures. *Crystallogr. Rev.* **2009**, *15*, 57–83, DOI: 10.1080/08893110802547240.

(51) Neese, F. The ORCA program system. *WIREs Comput. Mol. Sci.* **2012**, *2*, 73–78, DOI: 10.1002/wcms.81.

(52) Neese, F. Software update: the ORCA program system, version 4.0. *WIREs Comput. Mol. Sci.* **2018**, *8*, e1327, DOI: 10.1002/wcms.1327.

(53) Avogadro: an open-source molecular builder and visualization tool. Version 1.2.0. <http://avogadro.cc/>.

(54) Hanwell, M. D.; Curtis, D. E.; Lonie, D. C.; Vandermeersch, T.; Zurek, E.; Hutchison, G. R. Avogadro: an advanced semantic chemical editor, visualization, and analysis platform. *J. Cheminformatics* **2012**, *4*, 17, DOI: 10.1186/1758-2946-4-17.

